Acta Cryst. (1994). D**50**, 250–257

X-ray Structure of a Monoclinic Form of Hen Egg-White Lysozyme Crystallized at 313 K. Comparison of Two Independent Molecules

BY KAZUAKI HARATA

Biomolecules Department, National Institute of Bioscience and Human Technology, 1-1 Higashi, Tsukuba, Ibaraki 305, Japan

(*Received 27 September 1993; accepted 25 November 1993*)

Abstract

A monoclinic crystal of hen egg lysozyme (HEL, E.C. 3.2.1.17) was obtained at 313 K from a 10%(*w*/*v*) NaCl solution at pH 7.6 containing 5%(*v*/*v*) 1-propanol. Cell dimensions were $a = 27.23$, $b = 63.66$, $c = 59.12$ Å and $\beta = 92.9°$, and the space group was $P2_1$. The unit cell contains four molecules ($V_m = 1.79$ Å^3 Da^{-1}). The structure was solved by the isomorphous replacement method with anomalous scattering followed by phase improvement by the solvent-flattening method. The refinement of the structure was carried out by the simulated-annealing method. The conventional R value was 0.187 for 18 260 reflections [$|F_o| > 3\sigma(F)$] in the resolution range 10–1.72 Å. The r.m.s. deviations from the ideal bond distances and angles were 0.015 Å and 3.0°, respectively. The two molecules in the asymmetric unit are related by a translation of half a lattice unit along the a and c axes. The r.m.s. difference of equivalent C^α atoms between the two molecules was 0.64 Å and the largest difference was 3.57 Å for Gly71. A significant structural change was observed in the regions of residues 45–50, 65–73 and 100–104. The residues 45–50, which connect two β-strands, are shifted parallel to the β-sheet plane between the two molecules. The residues 100–104 belong to the substrate-binding site (subsite *A*) and the high flexibility of this region may be responsible for the binding of the substrate and the release of reaction products.

Introduction

Hen egg lysozyme (HEL) is a good example for investigating the ability of local structural change. The enzyme crystallizes in several crystal forms according to the difference in pH, temperature, reagents for crystallization, *etc.* (Steinrauf, 1959; Haas, 1967). High-resolution X-ray structures of triclinic (Ramanadham, Sieker & Jensen, 1990), monoclinic (Rao, Hoggle & Sundaralingam, 1983), orthorhombic (Berthou, Lifchitz, Artymiuk & Jolles, 1983) and tetragonal crystals (Blake *et al.*, 1965; Kundrot & Richards, 1987) have been reported. When a crystal contains two or more independent molecules, the structural difference can be seen under equivalent conditions. Monoclinic crystals of HEL contain two independent molecules in the asymmetric unit (Hogle *et al.*, 1981; Artymiuk, Blake, Rice & Wilson, 1982). In the presence of $NaNO_3$, two crystal forms were found depending on pH. The structure of the low-pH form has revealed that the two molecules are nearly identical at 2.5 Å resolution (Rao *et al.*, 1983). Alternatively, we have found that HEL crystallizes in a monoclinic form at 313 K in the presence of NaCl and 1-propanol. The X-ray diffraction data indicate that the crystal is similar to the high-pH form, the structure of which is unknown. The crystals diffract beyond 1.7 Å resolution and are suitable for high-resolution analysis to compare the structures of the two independent molecules.

Experimental

Crystallization and data collection

Hen egg lysozyme was purchased from Seikagaku Kogyo Co. and used without further purification. 1.0 g HEL was dissolved in 10 ml aqueous solution containing 10% NaCl and 5% 1-propanol. The pH of the solution was adjusted to 7.6 with 0.1 *N* HCl. The solution was allowed to stand at 313 K. Thick plate crystals appeared in a few days and were grown over two weeks. They belong to the monoclinic space group $P2_1$ with cell dimensions $a = 27.23$, $b = 63.66$, $c = 59.12$ Å, and $\beta = 92.9°$. The unit cell contains four molecules ($V_m = 1.79$ Å^3 Da^{-1}). The X-ray diffraction of the crystal, which was observed beyond 1.7 Å resolution, indicated the presence of pseudo-symmetry of the *B*-face centered lattice; the diffraction intensities of reflections with odd $h + l$ were considerably weaker than those of the other (even $h + l$) reflections, especially in the low-resolution range. Intensity data were collected on an Enraf–Nonius FAST diffractometer with a GX21 generator (40 kV, 60 mA, focal spot size 0.3 × 3 mm). Using three native crystals, three sets of independent reflections were obtained and were merged into a set

ISSN 0907-4449

of 18391 unique reflections that corresponds to 87.5% in the resolution range up to 1.72 Å. Statistics of the diffraction data are given in Table 1.

The heavy-atom solution was prepared using the mother liquor of the crystallization since crystals cracked in a freshly prepared solution. $HgCl_2$ (10 m*M*, 2 weeks) and $K_2Pt(CN)_4$ (5 m*M*, 8 d) were found to be effective for the preparation of heavy-atom derivatives. X-ray diffraction data were measured to 1.72 Å resolution in the same conditions that were used in the data collection of the native crystal. For each derivative, two crystals were used for data collection and two sets of reflection data were merged to produce a set of unique reflections.

Table 1. *Statistics of native data*

	Measured	Unique	R^*_{merge}
Crystal 1	31105	15478	0.110
Crystal 2	35607	15991	0.104
Crystal 3	36148	16153	0.102
Merge of three data sets		18391	0.061

* $R_{merge} = \sum[I(hkl)_j - G_j I(hkl)]/\sum I(hkl)_j$, where $I(hkl)$ is the average value of the observed intensities, $I(hkl)_j$, and G_j is the scale factor for the jth group.

Table 2. *Atomic parameters of heavy atoms*

	Occupancy*	*x*	*y*	*z*	*B* (Å^2)
$HgCl_2$ derivative					
Hg1	0.406	0.0500	0.2500	0.1547	19.3
Hg2	0.258	0.5442	0.2329	0.6367	24.3
Hg3	0.247	0.4931	0.0447	0.6255	17.4
Hg4	0.210	0.1941	0.1650	0.1966	20.9
Hg5	0.191	0.6970	0.1449	0.6731	21.7
$K_2Pt(CN)_4$ derivative					
Pt1	0.428	0.8660	0.0103	0.5370	22.4
Pt2	0.463	−0.0648	0.3588	0.0076	18.3
Pt3	0.395	0.4391	0.3510	0.5114	20.0

* Relative occupancy factor.

Structure determination and refinement

Main sites of the heavy atoms were determined by inspection of the difference Patterson map, and minor sites were found from the difference Fourier map in the course of refinement of the heavy-atom parameters. The average figure of merit was 0.58 for the reflections with $|F_o| > 3\sigma(F)$ within the resolution range 10–1.72 Å. The heavy-atom parameters are given in Table 2.

The electron-density map calculated with MIR phases did not reveal clearly the molecular boundary because of close packing of the molecule in the unit cell. The solvent-flattening technique (Wang, 1985) was applied to solve the problem. The solvent content was assumed to be 30% and the radius of the averaging sphere was set to 4 Å at the first stage. The reflections with $|F_o| > 3\sigma(F)$ in the resolution range 10–1.72 Å were used in the calculation. After six iterations, the figure of merit and the *R* value were 0.78 and 0.23, respectively. Then, the radius of the averaging sphere was reduced to 3 Å and solvent flattening and phase calculation were repeated three times. Finally, after five iterations with a radius of 2 Å, the figure of merit and the *R* value were 0.79 and 0.20, respectively. The average phase shift from the starting phases was 51.3°.

The electron-density map after the phase improvement by iterative solvent flattening was clear, and the amino-acid sequence was easily traced on the map. The HEL structure in the tetragonal crystal (Diamond, 1974) was placed in the unit cell so that the positions of the S atoms of the four disulfide bonds were fitted to those found on the map. Then, the position and orientation of the molecules were corrected by the rigid-body least-squares method (Scheringer, 1963). For 3813 reflections in the 10–3 Å resolution range, the *R* value was 0.455.

The structure was refined by the simulated-annealing method using the program *X-PLOR* (Brünger, Kuriyan & Karplus, 1987) at 10–1.72 Å. The molecular dynamics simulation was performed for 1 ps at 3000 K, 0.5 ps at 1000 K, and 0.5 ps at 300 K. The subsequent energy minimization for the coordinates (50 cycles) and *B* values (20 cycles) reduced the *R* value to 0.249. Water molecules were identified from Fourier and difference Fourier maps. Electron-density peaks higher than 5σ in the difference map were taken into account. The molecular dynamics calculation, including water molecules followed by the energy minimization, was repeated three times. During the dynamics calculation, the harmonic restraint (251 kJ mol^{-1} Å^{-2}) was imposed to water molecules. The temperature was lowered stepwise by in order of 2000 K (0.5 ps), 1000 K (0.5 ps), and 300 K (0.5 ps) for each run. After the energy minization at each stage, the Fourier and difference Fourier maps were examined and new water molecules were added whereas water molecules with the *B* value higher than 60 Å^2 were deleted. At the final stage of the refinement, 215 fully occupied water molecules were included in the structure model. The weight for the energy terms involving water molecules was reduced to 0.75 and the restraint weight for the *B* value was 0.02, which corresponds to 60% of the default value. The *R* value was 0.187 for 18260 reflections with $|F_o| > 3\sigma(F)$. The maximum values of negative and positive residual electron density were −0.45 and 0.59 e Å^{-3}, respectively. The r.m.s. residual electron density was 0.090 e Å^{-3} and no significant peak was found. The average values of r.m.s. deviations of bond distances and angles from their ideal values were 0.015 Å and 3.0°, respectively. The refined atomic coordinates have been deposited with Protein Data Bank,

Brookhaven.* Except for the program packages *ISIR* (Wang, 1985) and *X-PLOR* (Brünger *et al.*, 1987), computer programs used were those developed in the author's laboratory.

Results and discussion

Crystallization

The formation of monoclinic crystals with space group $P2_1$ was observed in the presence of $NaNO_3$. The cell dimensions of these crystals slightly differ depending on the pH of the mother solution. Hogle *et al.* (1981) observed marked differences in the X-ray diffraction patterns of crystals obtained at pH higher than 7.0 and crystals obtained at pH lower than 6.8. The high-pH crystals indicate the presence of pseudosymmetry of the *B*-centered lattice. The crystal used in the present structure analysis shows a diffraction pattern similar to that of the high-pH form. When the temperature is kept at 303–323 K, NaCl and 1-propanol cause an effect similar to that of $NaNO_3$. Only orthorhombic crystals of the high-temperature form (Berthou *et al.*, 1983) appeared in the absence of 1-propanol. At room temperature, only orthorhombic crystals of the high-pH form (Artymiuk *et al.*, 1982) were obtained even in the presence of 1-propanol. The present monoclinic crystal is stable at room temperature but does not grow. Therefore, the combination of NaCl and 1-propanol at 303–323 K is required to produce the present monoclinic crystal.

Structure determination and refinement

All heavy atoms are bound on the surface of the protein molecule. Hg2 and Hg4 are located near the residues Arg14 and His15 of molecule 1. Hg1 and Hg5 are found near the same residues in molecule 2. The $Pt(CN)_4^{2-}$ ion (Pt2 and Pt3) is located near the residues Tyr20 and Arg21 in both molecules. The positions of Hg2, Hg4 and Pt3 are related to the positions of Hg1, Hg5 and Pt2, respectively, by the pseudosymmetry of the *B*-centered lattice. These heavy atoms are located in a space between the two molecules related by the translation along the *a* axis. Hg3 is in the loop region Asn65–Ser72 in molecule 2 while Pt1 is near Arg128 of molecule 1. These two positions are found in a conformationally flexible region where the local structure differs between the two molecules.

As has been expected from the relatively low V_m value, protein molecules are closely packed in the crystal. In spite of the low solvent content (assumed to be 30%), the solvent-flattening method (Wang, 1985) improved the electron-density map. The average phase shift of 51.3° indicates that the multiple isomorphous replacement (MIR) phases have con-

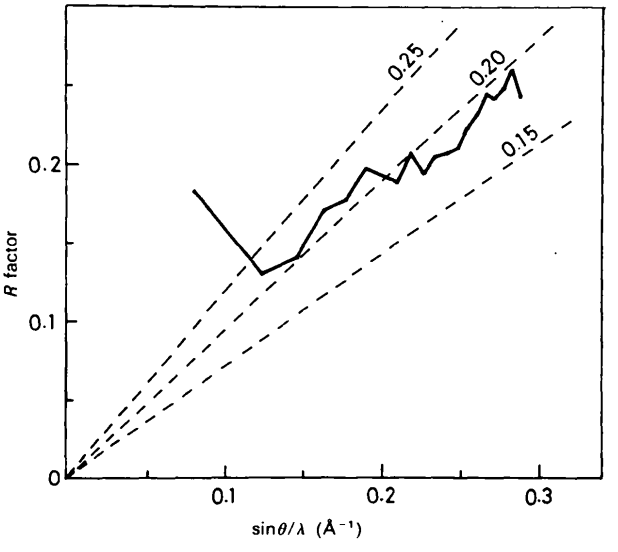

Fig. 1. Plot of the *R* factor as a function of $\sin\theta/\lambda$. Dashed lines are theoretical curves according to Luzzati (1952), which correspond to the upper estimate of coordinate errors of 0.15, 0.20 and 0.25 Å.

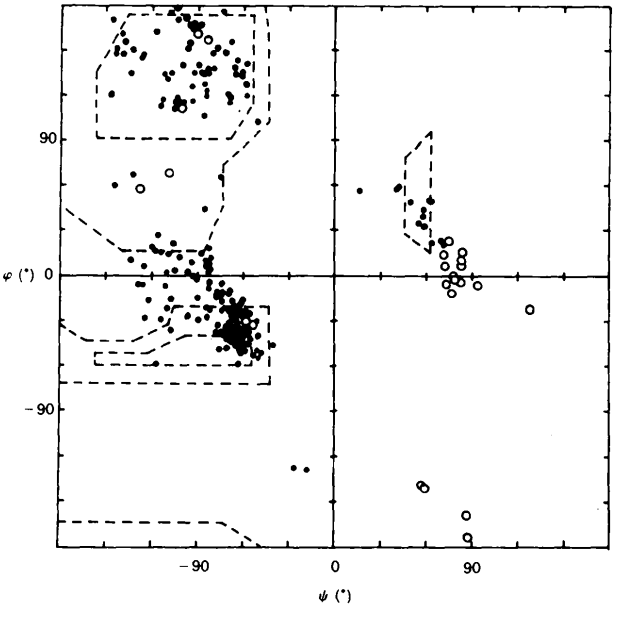

Fig. 2. Ramachandran plot for the main-chain torsion angles (φ,ψ) of molecule 1 and molecule 2. Glycine residues are shown as open circles.

* Atomic coordinates and structure factors have been deposited with the Protein Data Bank, Brookhaven National Laboratory (Reference: 1LYS, R1LYSSF). Free copies may be obtained through The Technical Editor, International Union of Crystallography, 5 Abbey Square, Chester CH1 2HU, England (Supplementary Publication No. SUP 37108). A list of deposited data is given at the end of this issue.

siderable error. A set of the protein coordinates of HEL in the tetragonal crystal (Diamond, 1974) was used as an initial model for the structure refinement. There were many polypeptide regions and side-chain groups showing disagreement between the model and the electron-density map. Such disagreement was corrected during the several iterations of the simulated-annealing procedure (Brünger *et al.*, 1987). The $2F_o - F_c$ map and $F_o - F_c$ map at the final stage confirmed that there is no significant disagreement between the model and the electron-density map. The R value is plotted against the resolution (Fig. 1). The coordinate error estimated by the Luzzati plot (Luzzati, 1952) is *ca* 0.2 Å. The Ramachandran map indicates that the (φ,ψ) values fall in the normal range although a deviation is observed for Pro70 and Arg128 in molecule 2 (Fig. 2).

Molecular structure

The basic folding of the polypeptide chain in molecules 1 and 2 is the same as that in the HEL structure found in the triclinic (Ramanadham *et al.*, 1990), monoclinic (Rao *et al.*, 1983) and tetragonal (Kundrot & Richards, 1987) crystals. The backbone structures of the two molecules are superimposed as shown in Fig. 3. The r.m.s. deviations between the equivalent atoms are 0.64 Å for the C^α atoms and 1.53 Å for all atoms. The plot of C^α difference is shown in Fig. 4. Sharp peaks are found at the residues Gly71 and Gly102. Disagreement is prominent in the loop regions 46–49 and 62–85. The region 46–49 connects two strands that form a β-sheet structure. As shown in Fig. 5, the end of the β-sheet is shifted parallel to the sheet plane. This β-sheet region forms a part of the active-site cleft and binds the substrate polysaccharide in cooperation with region 100–120. When the substrate analogue is bound, the cleft becomes narrower by the hinge bending motion. However, the present structure indicates that the β-sheet region moves parallel to the sheet plane in the absence of substrate. The comparison of (φ,ψ) angles indicates that the difference in the main-chain structure is prominent in the region of residues 45–50 (Table 3). The active center of HEL comprises Glu35 and Asp52. The Asp52 residue is located at the end of the β-strand. However, the lateral movement of the β-sheet does

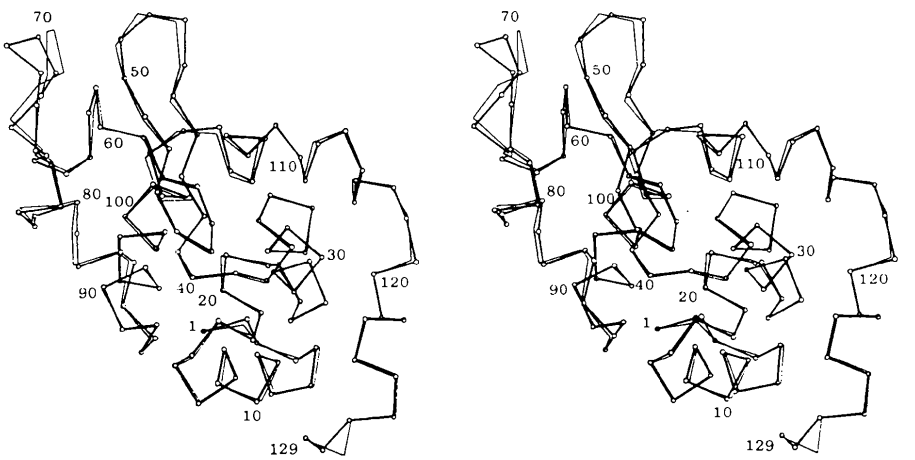

Fig. 3. Stereoview of the superposition of two molecules. C^α atoms in molecule 1 are shown by open circles.

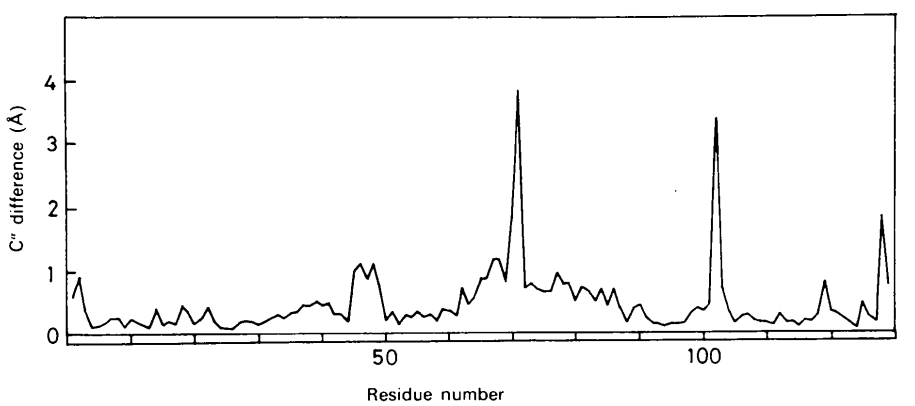

Fig. 4. Plot of the positional difference of equivalent C^α atoms.

not significantly affect the spatial relationship of these two residues. The side-chain group of Asp52 is in the same conformation and forms a hydrogen bond with the side chain of Asn59 in both molecules. The Glu35 residue in molecule 1 is also superimposed on the corresponding residue in the molecule 2.

The Trp62 residue has been considered to play an important role in substrate binding. The X-ray structures of the complex with oligosaccharides have shown that the pyranose ring of a sugar residue is bound parallel to the indole moiety by van der Waals forces (Blake *et al.* 1967; Cheetham, Artymiuk & Phillips, 1992; Strynadka & James, 1991; Ford, Johnson, Machin, Phillips & Tijan, 1974). The orientation of the indole group differs between the two molecules. The indole plane in molecule 1 is *ca* 180° rotated around the C^{β}—C^{γ} bond from the position found in molecule 2. Therefore, the side-chain group of Trp62 is highly flexible and may rotate in the absence of the substrate saccharide. The flexibility of the side-chain group is required to bind the substrate and to release the reaction product. The structural difference of this region is limited to the side-chain group and the polypeptide chain does not change significantly between the two molecules. The

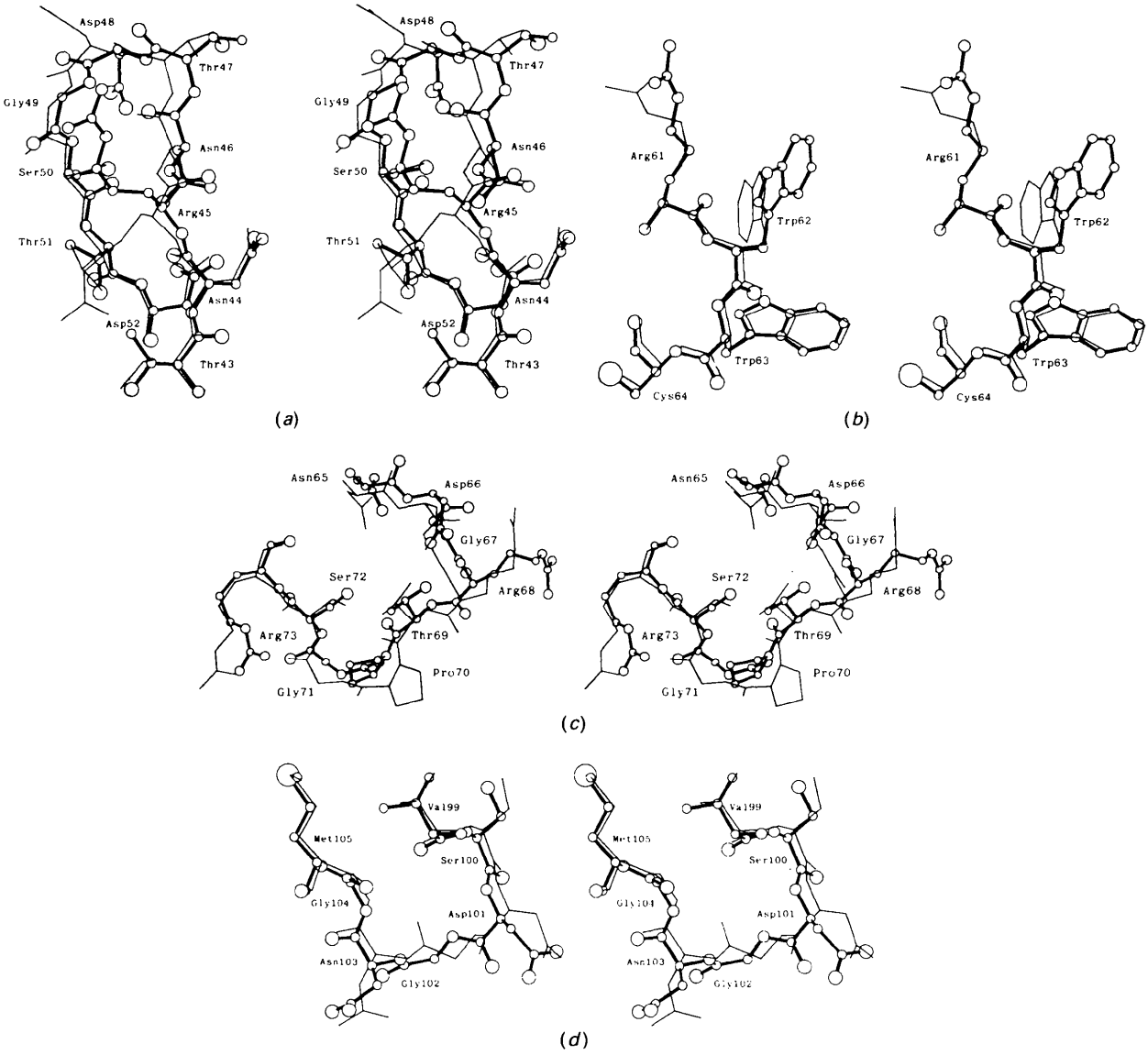

Fig. 5. Stereoviews of the superposition of local structures: Thr43–Thr51 (*a*), Arg61–Cys64 (*b*), Asn65–Arg73 (*c*), Val99–Met105 (*d*). Structures of molecule 2 are shown as thin lines.

Table 3. *Comparison of* (φ,ψ) *angles* (°)

	Molecule 1		Molecule 2		Triclinic		Tetragonal	
	φ	ψ	φ	ψ	φ	ψ	φ	ψ
Arg45	−84	123	85	135	93	116	92	142
Asn46	−103	179	−95	154	−94	158	−100	162
Thr47	−63	59	−51	32	−70	13	−62	−32
Asp48	−85	44	−81	7	−28	2	−76	−3
Gly49	72	6	94	8	96	−15	93	0
Ser50	−88	167	93	164	−88	158	−81	169
Gly67	79	3	73	−7	74	−1	69	10
Arg68	−133	10	−116	26	123	1	−134	18
Thr69	94	126	−142	151	−101	126	122	84
Pro70	−47	−52	17	−130	64	143	−42	127
Gly71	127	58	−108	68	74	23	60	46
Ser72	80	148	−72	176	−56	127	78	155
Arg73	117	162	106	175	−105	21	−100	10
Val99	−69	−24	69	−24	69	−26	−63	21
Ser100	−82	−9	84	9	−79	−28	−88	6
Asp101	−116	59	−90	3	−90	40	75	−3
Gly102	100	111	128	−24	75	19	118	−31
Asn103	17	57	110	8	−115	146	−102	12
Gly104	59	−142	57	141	−92	−155	58	−145

63rd residue is also Trp. However, the indole moiety of Trp63 is in the same orientation between the two molecules.

A loop region from Asn65 to Arg73 is most flexible in HEL as shown in Fig. 5. The largest difference is found in Gly71 where the positional difference of the C^{α} atom is 3.57 Å. The residues Thr69 and Pro70 also show large differences in the (φ,ψ) angles (Table 3). The structure of this region in both the molecules differs from those observed in the triclinic and the tetragonal crystals. The structural change affects the binding of heavy atoms. An Hg^{2+} ion is located between Asn65 and Thr69 in molecule 2. However, no Hg^{2+} ion is found in the corresponding site of molecule 1. This suggests that the loop structure of the 65–73 region in molecule 1 is not favorable for accommodation of the Hg^{2+} ion.

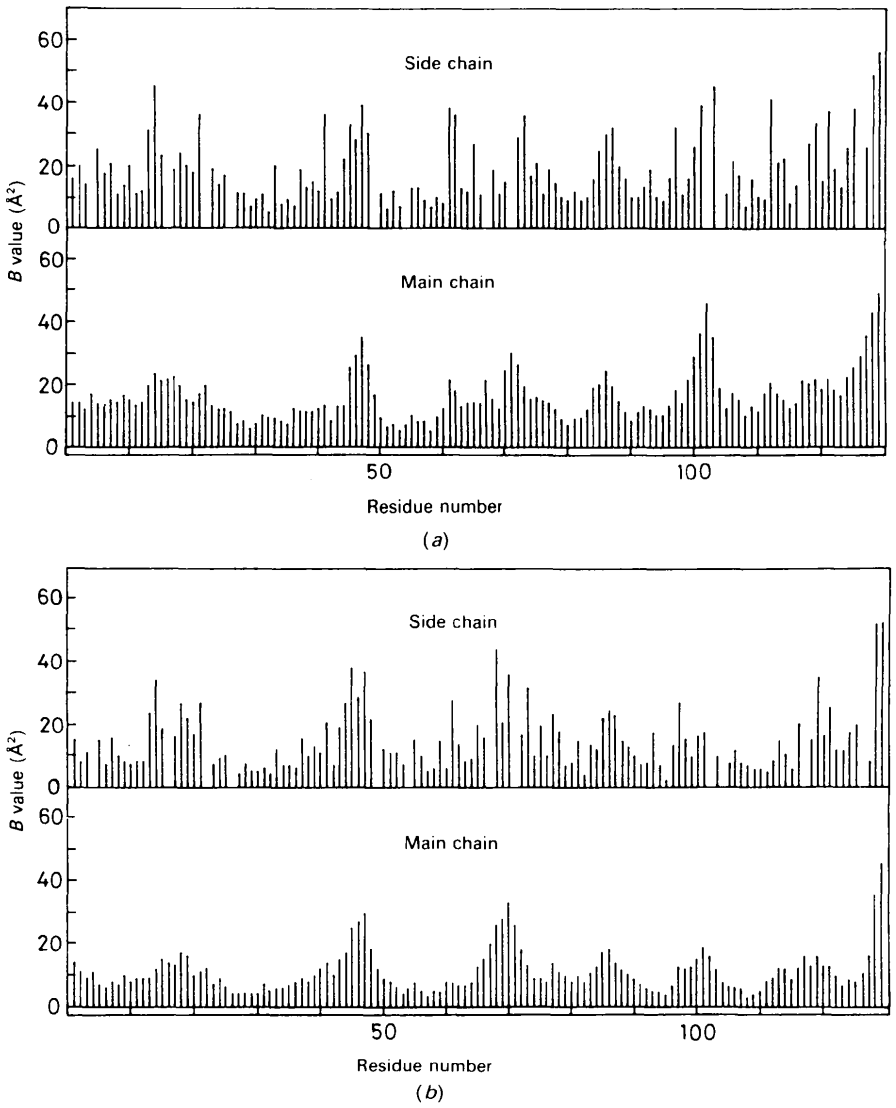

Fig. 6. Temperature factors averaged for the side chains and main chains in molecules 1 (*a*) and 2 (*b*).

A marked difference in the polypeptide structure is also observed in the region of residues Ser100–Gly104. This region binds the substrate saccharides and is called subsite *A*. The polypeptide conformation in molecule 2 is nearly the same as that of the tetragonal crystal. However, the structure of molecule 1 differs from that of the triclinic and tetragonal crystals. In the structure of the HEL complex with trisaccharide, the side-chain groups of Asp101 and Asn103 are hydrogen bonded to sugar residues (Cheetham *et al.*, 1992). The carboxymethyl group of Asp101 is in the same conformation in molecule 1 and molecule 2. However, the side-chain group of Asn103 is oriented in the opposite direction in the two molecules. This suggests that the structure of subsite *A* is flexible in the absence of substrate. The side-chain groups are oriented so that they may not interfere with the insertion of the saccharide substrate into the active-site cleft. The accommodation of the substrate induces a structural change of this region to fix the sugar residues by hydrogen bonds involving Asp101 and Asn103.

The average *B* values for peptide and side-chain groups are plotted against the residue number in Fig. 6. The average values for molecules 1 and 2 are 18.2 and 13.6 Å^2, respectively. The *B* value of molecule 1 is considerably larger than that of molecule 2. The average *B* values for main chains and side chains are 16.0 and 20.4 Å^2 for molecule 1 and 11.3 and 16.1 Å^2 for molecule 2, respectively. The region having large *B* values coincides with the region where the prominent structural change is observed between the two molecules. The profile of the *B* value plot is similar in the two molecules. A significant difference is observed in the region of residues 99–103. Relatively large *B* values are observed in molecule 1 while *B* values of the corresponding region in molecule 2 are less than 20 Å^2.

The HEL structure in solution has been investigated by NMR spectroscopy (Smith, Sutcliffe, Redfield & Dobson, 1993). The structures of well defined regions in solution are very similar to those observed in the crystalline state. A relatively large r.m.s. deviation from the mean structure is observed in the region of residues 46–69 and 68–70 which are found to be the most movable regions in the present X-ray structure. The side-chain conformation of Trp62 is almost completely disordered in the structure. The structure of each individual molecule in the crystal can be considered as a snapshot of the dynamic state. Then, the combination of several snapshots will give an insight into the nature of the dynamic structure in solution.

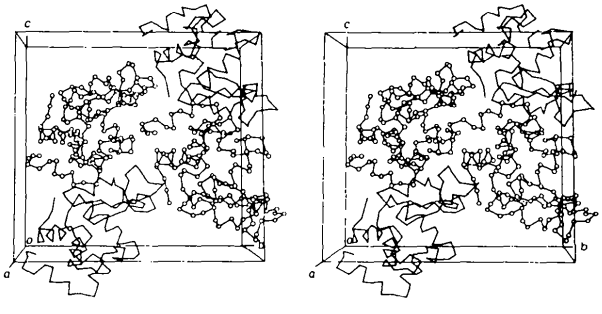

Fig. 7. Stereoview of the crystal packing. C$^\alpha$ atoms in molecule 1 are shown as open circles.

Crystal packing

The crystal structure is shown in Fig. 7. The packing structure resembles the structure of the low-pH form obtained in the presence of $NaNO_3$ (Rao *et al.*, 1983). The two independent molecules are related by a translation of half a lattice unit along the *a* and *c* axes. Molecule 1 is superimposed on molecule 2 by the following equation

$$x' = 0.9988x - 0.0425y + 0.0241z + 14.998$$

$$y' = 0.0406x + 0.9966y + 0.0714z + 0.982$$

$$z' = -0.0271x - 0.0703y + 0.9972z - 29.191.$$

Because of the close packing of the molecules in the crystal, there are many intermolecular contacts involving hydrogen bonds or salt linkages. Most of intermolecular contacts involve flexible regions in the molecule, which include residues 46–49, 65–73 and 100–104. These are regions which are also involved in intermolecular contacts in the triclinic and tetragonal crystals. The local structure of these regions differs between the monoclinic, triclinic and tetragonal crystals. This suggests that the conformational difference at the molecular surface reflects the crystal packing. It is plausible that several molecular species, among which the local structure of some flexible regions differ, are in equilibrium in solution. The conformational variability found in regions involving intermolecular contacts may provide a driving force to produce a variety of crystal forms.

The author thanks Dr M. Muraki for his aid with carrying out the structure refinement by *X-PLOR* on an IRIS4D computer.

References

ARTYMIUK, P. J., BLAKE, C. C. F., RICE, D. W. & WILSON, K. S. (1982). *Acta Cryst.* **B38**, 778–783.

BERTHOU, J., LIFCHITZ, A., ARTYMIUK, P. J. & JOLLES, P. (1983). *Proc. R. Soc. London Ser. B*, **217**, 471–489.

BLAKE, C. C. F., JOHNSON, L. N., MAIR, G. A., NORTH, A. C. T., PHILLIPS, D. C. & SARMA, V. R. (1967). *Proc. R. Soc. London Ser. B*, **167**, 365–377.

BLAKE, C. C. F., KOENIG, D. F., MAIR, G. A., NORTH, A. C. T., PHILLIPS, D. C. & SARMA, V. R. (1965). *Nature (London)*, **206**, 757–763.

BRÜNGER, A. T., KURIYAN, J. & KARPLUS, M. (1987). *Science*, **235**, 458–460.
CHEETHAM, J. C., ARTYMIUK, P. J. & PHILLIPS, D. C. (1992). *J. Mol. Biol.* **224**, 613–628.
DIAMOND, R. (1974). *J. Mol. Biol.* **82**, 371–391.
FORD, L. O., JOHNSON, L. N., MACHIN, P. A., PHILLIPS, D. C. & TJIAN, R. (1974). *J. Mol. Biol.* **88**, 349–371.
HAAS, D. J. (1967). *Acta Cryst.* **23**, 666.
HOGLE, J., RAO, S. T., MALLIKARJUNAN, M., BEDDELL, C., MCMULLAN, R. K. & SUNDARALINGAM, M. (1981). *Acta Cryst.* B**37**, 591–597.
KUNDROT, C. E. & RICHARDS, F. M. (1987). *J. Mol. Biol.* **193**, 157–170.
LUZZATI, V. (1952). *Acta Cryst.* **5**, 802–810.
RAMANADHAM, M., SIEKER, L. C. & JENSEN, L. H. (1990). *Acta Cryst.* B**46**, 63–69.
RAO, S. T., HOGGLE, J. & SUNDARALINGAM, M. (1983). *Acta Cryst.* C**39**, 237–240.
SCHERINGER, C. (1963). *Acta Cryst.* **16**, 546–550.
SMITH, L. J., SUTCLIFFE, M. J., REDFIELD, C. & DOBSON, C. M. (1993). *J. Mol. Biol.* **229**, 930–944.
STEINRAUF, L. K. (1959). *Acta Cryst.* **12**, 77–79.
STRYNADKA, N. C. & JAMES, M. N. G. (1991). *J. Mol. Biol.* **220**, 401–424.
WANG, B.-C. (1985). In *Methods in Enzymology*, Vol. 115, edited by H. W. WYCKOFF, C. H. W. HIRS & S. N. TIMASHEFF, pp. 90–112. London: Academic Press.